Fluoride-activated Catalysis

Tsygankov, Aleksei

DOI:
10.33612/diss.587515831

Chapter 3:
Reductive α-Alkylation of Ketones with Aldehydes at Atmospheric Pressure of Carbon Monoxide

This chapter describes the reductive alkylation of ketones with aldehydes using carbon monoxide as a reducing agent. The use of fluoride additive in the present protocol allows to achieve milder conditions compared to the previously reported one. The role of the fluoride additive in this transformation has been investigated procedure and a probable explanation was provided.

Part of this chapter has been published:

S. A. Runikhina, A. Tsygankov, O. I. Afanasyev, and D. Chusov, *Mendeleev Commun* **2023**, *33*, 17-20

3.1. Introduction

Direct α-modification of ketones is highly demanded in the synthesis of drug substances.[1] The classical approach to this transformation implies the use of alkyl halides in the presence of a base (Figure 13a). This reaction suffers from the low atom economy and in some cases serious cancerogenic toxicity of the alkyl halides. The possible solution to this problem is the reductive alkylation reaction (Figure 13b). Usually, this is a two-step protocol in which the α,ß-unsaturated carbonyl compound is formed in the first step followed by its reduction. However, the selective hydrogenation of α,ß-unsaturated carbonyl compounds could be a problem. Such reactions might suffer from the over-reduction of different functionalities in the molecule.

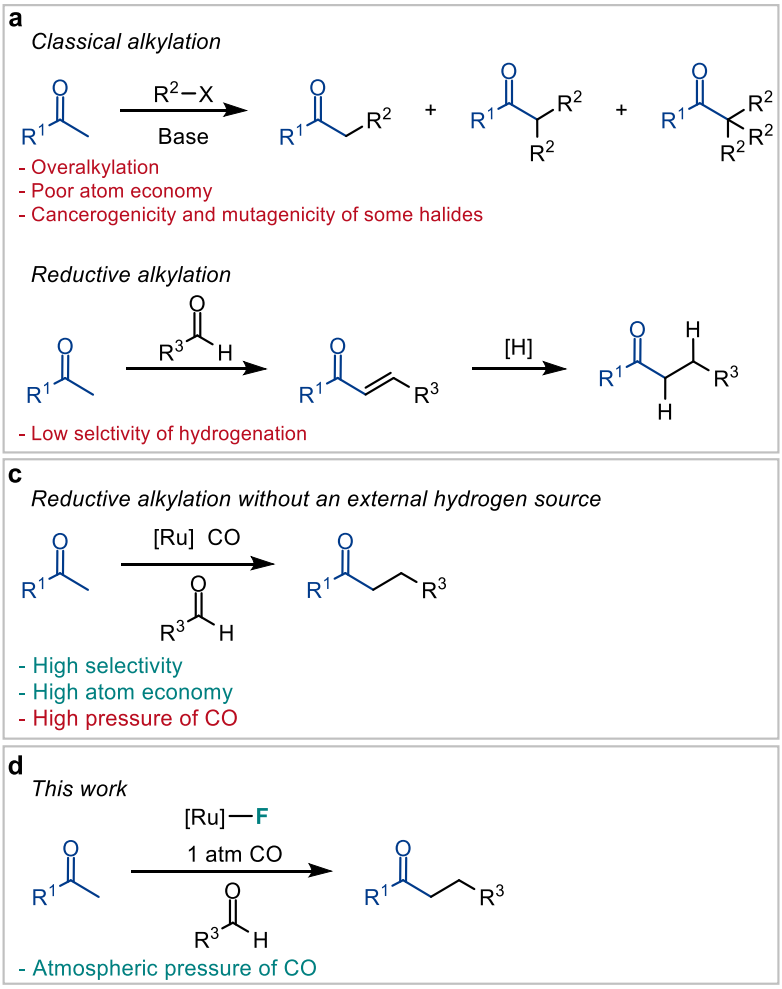

Figure 13. α-Modification of ketones. **a**. Traditional approaches for α-alkylation of ketones. **b**. Previous work of our group on reductive alkylation using carbon monoxide as a reducing agent. **c**. Reductive alkylation of ketones using atmospheric pressure of carbon monoxide enabled by fluoride activation of the ruthenium catalyst.

Earlier our group developed the ruthenium-catalyzed reductive a-alkylation of ketones with aldehydes without an external hydrogen source (Figure 13c).[2] This reaction was catalyzed by [(*p*-cymene)$RuCl_2$]$_2$, a simple and readily available ruthenium source. The high selectivity of this process is caused by the use of CO, a highly selective reducing agent for some transformations, such as reductive amination, amidation and esterification of carbonyl compounds.[3–10] However, in a general case an elevated pressure of CO is required to achieve the preparative yield of the product. Herein we demonstrated that the application of the fluoride activation approach allowed us to carry out this reaction at one atmosphere of carbon monoxide (Figure 13d).

3.2. Results and Discussion

The optimization was carried out using a reaction for the preparation of the industrially valuable nonsteroidal anti-inflammatory drug Nabumetone.[11] In the previous work, our group succeeded to prepare this compound using 10 atm CO at 200 °C and [(*p*-cymene)$RuCl_2$]$_2$ as a catalyst.[2] In this paper, our goal was to develop a useful protocol working without autoclaves at one atmosphere of carbon monoxide.

We compared the activity of the ruthenium catalyst under much milder conditions than the ones used before (Table 1). Without additives, the reductive aldol reaction proceeded with a low efficiency providing a product with only 16% yield (entry 1). The addition of $Bu_4N(Ph_3SiF_2)$ (TBAT), a stable and soluble in organic solvents fluoride source, led to a more than twice increase in the yield (entry 2). The addition of Bu_4NF (TBAF), as an alternative source of fluoride, had a less prominent effect (entry 3), which may be explained by the high hygroscopicity of this salt. Water could potentially interrupt the reaction. The use of tetrabutylammonium chloride (TBAC), bromide (TBAB), or iodide (TBAI) (entries 4–6) resulted in a two- or fourfold decrease in the yield.

Encouraged by the result obtained when TBAT was used as an additive we decided to study the effect of the amount of the additive on the yield. The product yield depended almost linearly on the TBAT concentration (Figure 14). The best results were obtained with 16% of the TBAT. A further increase in the amount of TBAT was not impractical since it would make the isolation of the product from the reaction mixture more difficult. Therefore, it was necessary to investigate for other ways to increase the yield of the reaction product.

Table 7. Additive screening for reductive alkylation.

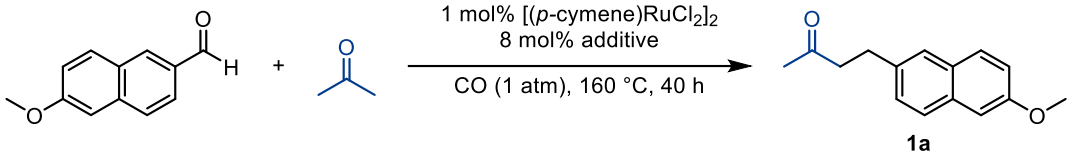

Entry[a]	Additive	Yield[b] (%)
1	-	16
2	TBAT	39
3	TBAF	22
4	TBAC	5
5[a]	TBAB	7
6	TBAI	8

[a] Reaction conditions: 6-methoxy-2-naphthaldehyde (0.4 mmol), acetone (3.5 ml), [(*p*-cymene)$RuCl_2$]$_2$ (1 mol%), additive (8 mol%). The reactions performed in a 100 ml screw-cap Schlenk tube. Depth of the Schlenk tube immersion into the oil bath – 4/5. [b] Yields were determined by ^{1}H NMR.

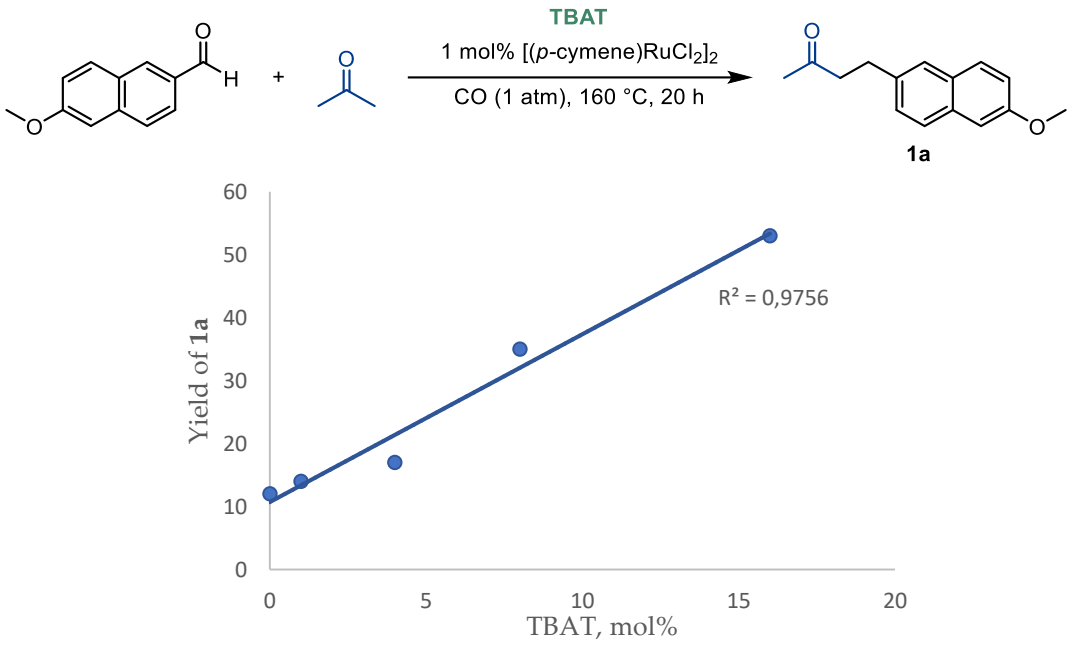

Figure 14. Dependence of yield on the TBAT concentration.

Varying of the catalyst loading (Table 2, entries 1-4) or the reaction (entries 5-7) temperature did not lead to an increase in the product yield. Unexpectedly, the important parameter for the reaction efficiency was the depth of immersion of the Schlenk tube into the oil bath (entries 8 and 9). When the depth of immersion of the Schlenk tube was 3/5, product **1a** was obtained in high and reproducible yield. It seems that under these conditions, optimal concentrations of the system components in a 100 ml Schlenk tube are achieved. Changing the depth of immersion results in a change of

concentration of acetone since some of it is going into the gas phase which has influence on overall pressure inside the Schlenk tube during the reaction which on its turn influences the solubility of the CO in the solvent. The drawback of this systems is that reaction conditions unfortunately are highly dependent on the type of the reaction vessel, and it will require additional optimization for conducting these reactions on different scales using Schlenk tubes with other volumes.

Table 8. Screening of reaction conditions.

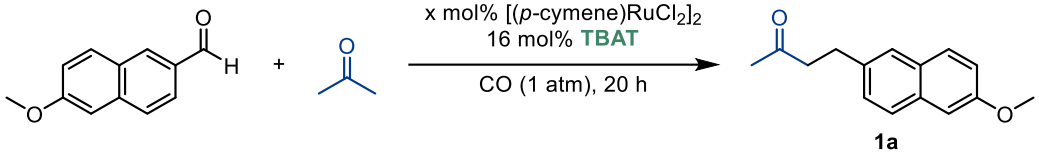

Entry[a]	Catalyst loading (mol%)	T, °C	Yield[b] (%)
1	0	160	0
2	0.5	160	49
3	1	160	53
4	2	160	26
5[a]	1	140	46
6	1	150	52
7	1	170	43
8[c]	1	160	92
9[d]	1	160	80

[a] Reaction conditions: 6-methoxy-2-naphthaldehyde (0.4 mmol), acetone (3.5 ml), [(*p*-cymene)$RuCl_2$]$_2$ (1 mol%), TBAT (16 mol%). The reactions performed in a 100 ml screw-cap Schlenk tube. Depth of the Schlenk tube immersion into oil bath – 4/5. [b] Yields were determined by ^{1}H NMR. [c] Depth of the Schlenk tube immersion into oil bath – 3/5. [d] Depth of the Schlenk tube immersion into oil bath – 1/5.

The advantage of using acetone as one of the reagents in reductive alkylation is that it can be used in excess. In this case, acetone acts both as a reagent and as a solvent. At the end of the reaction excess of the acetone can be easily removed. However, this is not optimal when more complex ketones are used because, in this case, it would be hard to isolate the product from the excess of the ketone. In the previous work on reductive alkylation (Figure 13b), the use of THF as a solvent was found to be optimal.[2] Therefore, to obtain product **1b** from aromatic aldehyde and aromatic ketone we used THF as a solvent. We tested different concentrations of the substrates in THF (Table 9, entry 1-3) and different depths of the immersion of the Schlenk tube in the oil bath (entries 3 and 4). As a result, we were able to obtain product **1b** in 70% NMR yield (entry 4).

Table 9. Optimization of the reaction conditions using aromatic ketone as a substrate.

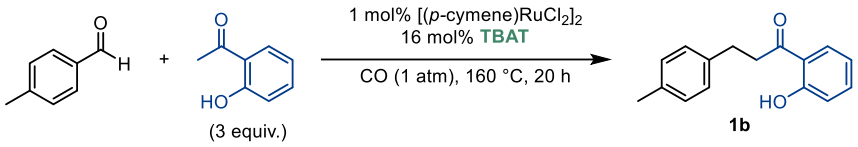

Entry[a]	Concentration of aldehyde	Depth of immersion	Yield[b]
1	0.11 M	3/5	10%
2	0.27 M	3/5	59%
3	0.40 M	3/5	50%
4	0.27 M	4/5	70%

[a] Reaction conditions: 4-methylbenzaldehyde (0.4 mmol, 1 equiv.), 2′-hydroxyacetophenone (1.2 mmol, 3 equiv.), THF, [(p-cymene)$RuCl_2$]$_2$ (1 mol%), TBAT (16 mol%), the reactions were performed in a 100 ml screw-cap Schlenk tube. [b] Yields were determined by ^{1}H NMR.

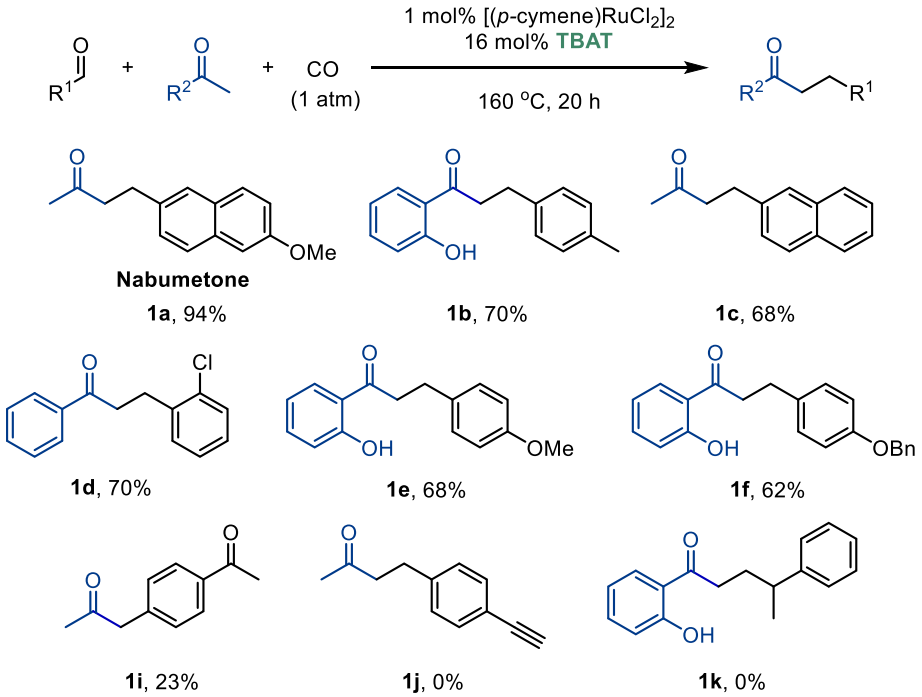

Figure 15. Substrate scope for reductive alkylation. Reaction conditions: For substrates prepared by alkylation of acetone: aldehyde (0.4 mmol), acetone (4.7 ml), [(*p*-cymene)$RuCl_2$]$_2$ (1 mol%), TBAT (16 mol%), 100 ml screw-cap Schlenk tube, depth of the Schlenk tube immersion into oil bath – 3/5. For substrates prepared by alkylation of acetophenone derivatives: aldehyde (0.4 mmol), ketone (1.2 mmol), [(p-cymene)$RuCl_2$]$_2$ (1 mol%), TBAT (16 mol%), THF (1.5 ml), 100 ml screw-cap Schlenk tube. depth of the Schlenk tube immersion into the oil bath – 4/5. Yields were determined by ^{1}H NMR or GC.

Having optimized the reaction conditions for two different ketones we proceeded to the substrate scope study (Figure 13). Both aliphatic and aromatic ketones can be used in this transformation. Phenol moiety does not block the reaction (**1b**, **1e, 1d**).

Altogether, these data indicate that the developed protocol could be considered a useful tool for ketone alkylation. For example, in view of medicinal chemistry, substrate **1b** is the direct precursor for the compound with anticancer activity comparable to Cisplatin.[12] The proposed method has some limitations. Reaction with 4-acetylbenzaldehyde led to a complex mixture of products with only 23% of the desired product **1i**. This is caused by the presence of three CH groups susceptible to alkylation by aldehyde. In the presence of the terminal alkynyl group, a polymeric product was formed with no signs of **1j**. Aliphatic aldehyde also does not allow to get the **1k** leading to the formation of a complex mixture of unidentified compounds mostly likely caused by self-aldol condensation of the aldehyde.

To check the possible reasons for the activation of the ruthenium catalyst by fluoride control experiments were carried out. First, NMR experiments were conducted (Scheme 32). No reaction occurred between TBAT and [(*p*-cymene)$RuCl_2$]$_2$ at 45 °C during the 2 hours in argon atmosphere (Scheme 32a). In the presence of carbon monoxide at 45 °C, the signals from the [(*p*-cymene)$RuCl_2$]$_2$ disappeared immediately suggesting the formation of the ruthenium carbonyl complex (Scheme 32b). TBAT had not reacted at these conditions. On the other hand, at 160 °C full conversion of TBAT and ruthenium complex is observed (Scheme 32c). TBAT is converted to Ph_3SiF thus releasing one equivalent of F^- which we believe is connected to the ruthenium complex. However, ruthenium fluoride complexes were not detected by ^{19}F NMR.

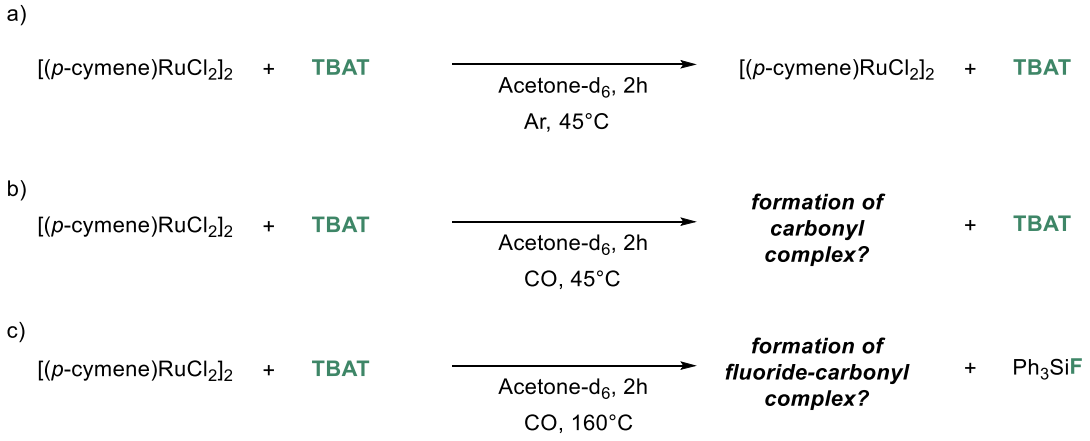

Scheme 32. Control experiments studied with NMR.

We then analyzed similar reaction mixtures using ESI-MS (Scheme 33). The reaction of [(*p*-cymene)$RuCl_2$]$_2$ with CO in the absence of TBAT led to the formation of mixtures of ruthenium carbonyl chloride complexes which is in the accordance with literature data (Scheme 33a).[13,14] The main particle detected in the solution by ESI-MS was $Ru(CO)_3Cl_3^-$ (**2**). In the presence of TBAT in addition to the formation of $Ru(CO)_3Cl_3^-$ (**2**) several mixed chloride-fluoride oligomeric carbonyl complexes (**4**) were detected

containing two to four ruthenium atoms (Scheme 33b). The formation of such oligomeric fluoride ruthenium complexes is in line with other literature reports.[15,16]

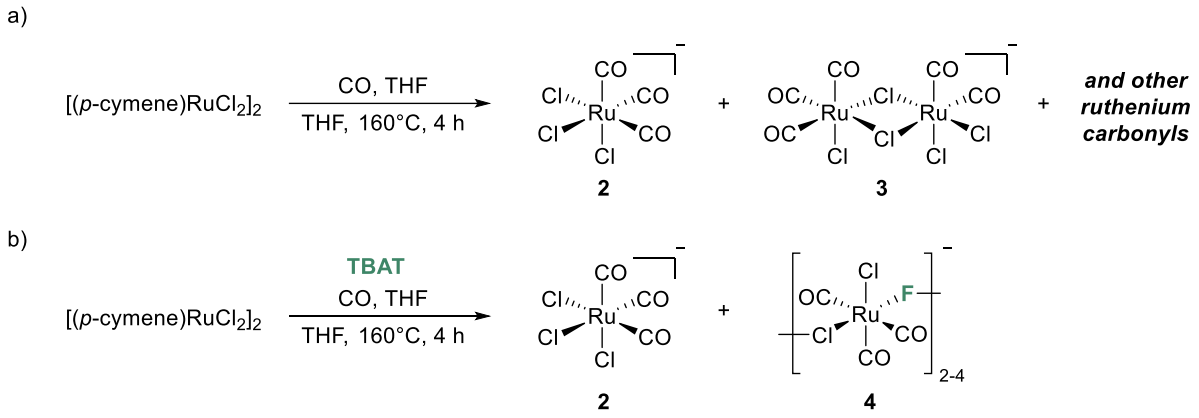

Scheme 33. Species identified by ESI-MS in a) absence of the additive, b) in the presence of TBAT

Based on these data and previous results of our group[2,17,18] as well as the literature reports we propose the possible mechanism for the reaction and the explanation of the role of fluoride in this process (Scheme 34). We assume that the oligomeric ruthenium halide complexes with $18e^-$ configuration are the catalyst resting states. Their depolymerization gives the catalytically active $16e^-$ complex **A**. Due to the fluorine coordination, the electrophilicity of the ruthenium center is increased, which facilitates the ketone coordination to the metal center. In the resulting intermediate **B,** the fluoride ligand acts as a hydrogen bond acceptor [15,16] helping to deprotonate the α-position of the ketone to give an intermediate **C**. In the next stages, fluoride may serve as a proton-transfer mediator or as a hydrogen bond acceptor for the precoordination of different molecules. In intermediate **D**, the aldehyde is coordinated to HF followed by an attack of enolate to give an intermediate **E**. The resulting aldol coordinates the ruthenium in a bidentate mode with HF transfer to the outer sphere to give **F**. HF-assisted H_2O elimination gives the intermediate **G** in which the inner-sphere CO to COOH oxidation followed by CO_2 evolution and cyclometallation step leads to the particle **J**. In the presence of HF, this complex is transformed to **K**, and the latter after the product to CO exchange regenerates the starting particle **A**. It should be noted that it is a putative mechanism and additional mechanistic studies with control experiments and theoretical calculations are required to validate the mechanism.

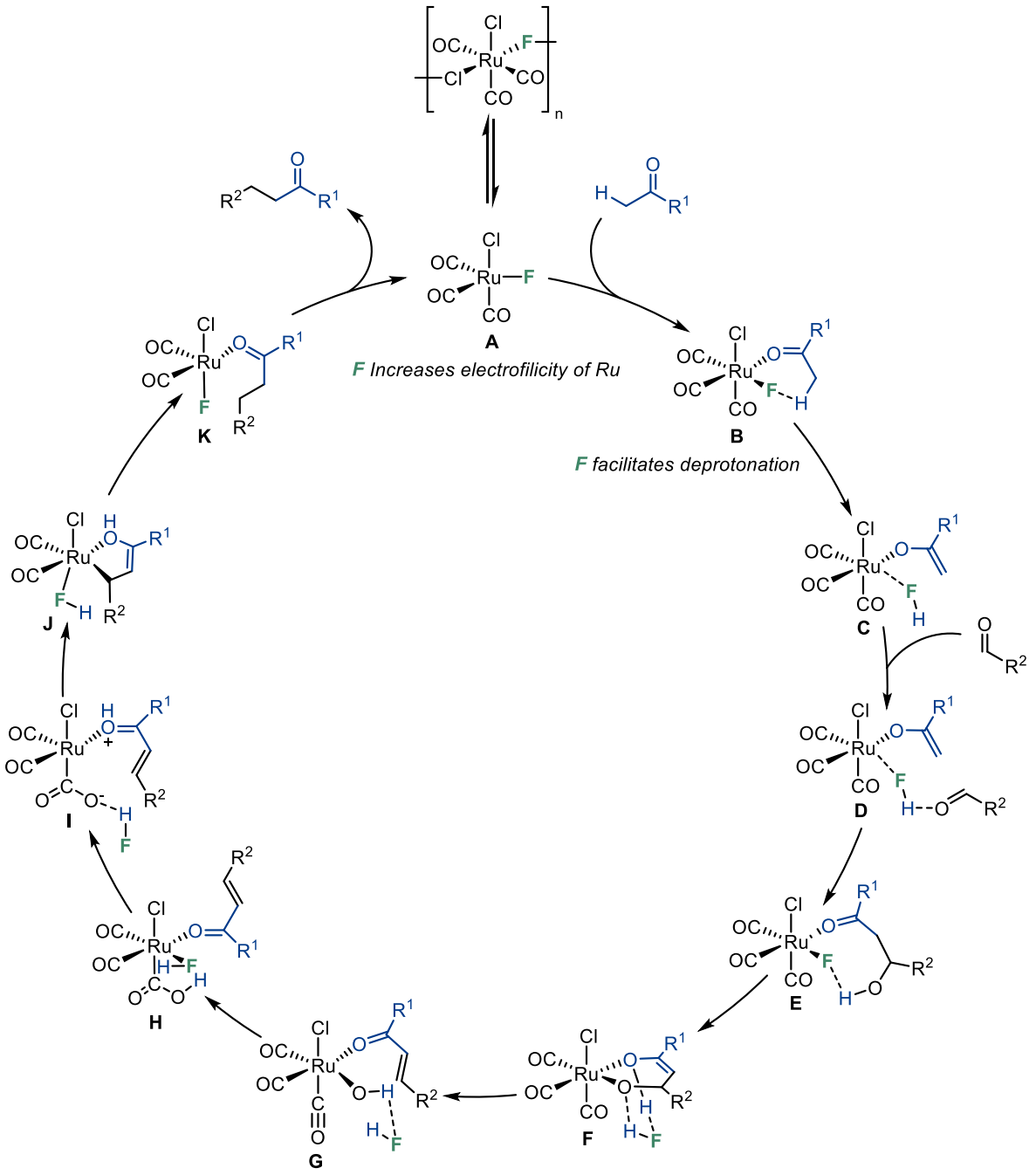

Scheme 34. Proposed mechanism.

3.3. Conclusion

We have demonstrated that activation of ruthenium catalyst with fluoride additive can lead not only to an increased activity but also to the use of milder reaction conditions. Using a fluoride source to activate the ruthenium catalyst allowed us to carry out the reductive alkylation of ketones by aldehydes at 1 atmosphere of CO, while the previously reported version of this reaction required 5-50 atmospheres to achieve preparative yields of the product. Explanation for the fluoride activation of the catalyst

was suggested. The strong electron-withdrawing ability of the fluoride increases the Lewis acidity of the metal. The possibility of fluoride to form the hydrogen bonds and thus mediate the proton transfer steps of the mechanism. An industrially valuable drug substance, Nabumetone, was prepared in a high yield.

3.4. Experimental section

3.4.1. General information

Unless otherwise stated, all reagents were purchased from commercial suppliers and used without further purification, THF and Et_2O were distilled over sodium/benzophenone, DCM was distilled over calcium hydride, acetone was dried over 3Å MS, MeCN was taken from a dry solvent purification system (SPS) machine. Carbon monoxide obtained from NII KM (Moscow, Russia). Purification of the products was performed either via column chromatography (Acros Organic silica gel 0.06–0.2 mm) or using an MPLC machine InterChim PuriFlash with PF-30SIHP- F0012 column. For other details of the chromatographic procedures, see the descriptions of the particular compounds below.

NMR spectra were recorded on Bruker Avance 300, Bruker Avance 400, and Varian Inova 400 operating at the denoted spectrometer frequency given in MHz for the specified nucleus. Peaks were referenced to residual solvent. The following abbreviations were used to designate chemical shift multiplicities: s = singlet, d = doublet, t = triplet, q = quartet, m = multiplet, br = broad; coupling constants are given in Hertz (Hz).

Analytical gas chromatography (GC) was performed using a Chromatec Crystal 5000.2 gas chromatograph fitted with a flame ionization detector (He was used as the carrier gas, 37 mL/min) and an MS detector. Chromatec CR-5MS (30 meters) capillary column was used. GC settings for the yield determination using the FID detector and the CR5ms column: the injector temperature was 250 °C, the split ratio of 50:1 at the moment of injection, and the FID temperature was 250 °C. Column compartment temperature program: 100°C for 2 min, 100°C → 280°C at 30°C/min, 280°C for 3 min. GC yields were determined with dodecane internal standard. For GC-MS analysis: the injector temperature was 250 °C, split ratio of 75:1 at the moment of injection. Column compartment temperature program: 60°C for 4 min, 60°C → 250°C at 30°C/min, 250°C for 12 min. Flow rate 1 mL/min. MSD parameters: ion source temperature 200°C, transfer line temperature 230°C. ESI-MS spectra were registered using LC-MS-2020 (Shimadzu). The voltage on the capillary was 4500 V; the range of scanned masses, m/z was 50-2000. Nitrogen as dry gas (15 l/min) and nebulizer gas (1.5 l/min); interface

temperature: 150 °C, heat block temperature 150°C, flow rate 0.1 ml/min (acetonitrile as an eluent, direct connection of LC and MS modules without column).

3.4.2. General procedure for reductive alkylation with acetone

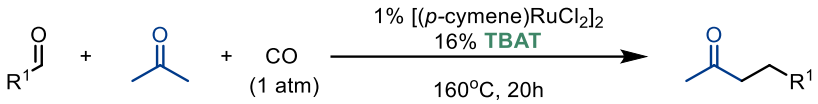

A 100 mL screw-cap Schlenk tube equipped with a stirring bar was dried by Schlenk technique and charged 2.5 mg [(*p*-cymene)$RuCl_2$]$_2$ (4 μmol, 1 mol%), 34.6 mg of TBAT (64 μmol, 16 mol%), and 1 mL of dry DCM. The solution was stirred for 15 minutes, then the solvent was evaporated from the Schlenk tube, and the vessel was filled with carbon monoxide. Aldehyde (0.4 mmol, 1 equiv.) and acetone (4.7 ml) were added in the carbon monoxide flow. The Schlenk tube was sealed and placed merged on 3/5 into a preheated oil bath to 160 °C. The reaction mixture was transferred into a flask and the Schlenk tube was washed with dichloromethane (2x3ml) and solvents were removed on a rotary evaporator. After the indicated time, the reactor was cooled to room temperature. The residue was analyzed using NMR or GC, and the product was isolated using chromatography (preparative TLC, column chromatography on silica gel, or using flash chromatograph InterChim PuriFlash).

3.4.2. General procedure for reductive alkylation with acetophenone derivatives

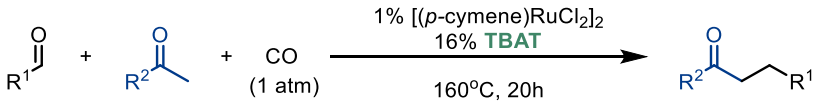

A 100 mL screw-cap Schlenk tube equipped with a stirring bar was dried by Schlenk technique and charged 2.5 mg [(*p*-cymene)$RuCl_2$]$_2$ (4 μmol, 1 mol%), 34.6 mg of TBAT (64 μmol, 16 mol%), and 1 mL of dry DCM. The solution was stirred for 15 minutes, then the solvent was evaporated from the Schlenk tube, and the vessel was filled with carbon monoxide. Aldehyde (0.4 mmol), ketone (1.20 mmol), and 1.50 mL of dry THF were added in the carbon monoxide flow. The Schlenk tube was sealed and placed merged on 4/5 into a preheated oil bath to 160 °C. After 20 hours, the reactor was cooled to room temperature. The reaction mixture was transferred into a flask and the Schlenk tube was washed with dichloromethane (2x3mL) and solvents were removed on a rotary evaporator. The residue was analyzed using NMR or GC, and the product was isolated using chromatography (preparative TLC, column chromatography on silica gel, or using flash chromatograph InterChim PuriFlash).

3.4.3. Spectroscopic and analytical data

4-(6-Methoxynaphthalen-2-yl)butan-2-one (1a)

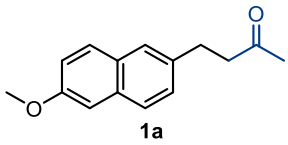

1a

Following the general procedure for the reductive alkylation with acetone using 76.0 mg of 6-methoxy-2-naphthaldehyde (0.41 mmol) product **1a** was obtained in 94% NMR yield. The residue was purified by preparative thin-layer chromatography (eluent: hexane: ethyl acetate 3:1; Rf=0.63) to afford 83.0 mg (89%) of the product as yellow crystals.

^{1}H NMR (400 MHz, Chloroform-d) δ 7.68 (two dd appears as d, *J* = 8.5 Hz, 2H), 7.55 (dd appears as broad s, 1H), 7.29 (dd appears as d, *J* = 8.3, 1H), 7.19 – 7.07 (m, 2H), 3.90 (s, 3H), 3.03 (t, *J* = 7.6 Hz, 2H), 2.83 (t, *J* = 7.6 Hz, 2H), 2.15 (s, 3H).
^{13}C NMR (101 MHz, Chloroform-d) δ 208.1, 157.3, 136.2, 133.1, 129.1, 129.0, 127.6, 127.0, 126.3, 118.9, 105.7, 55.3, 45.3, 30.2, 29.8.
NMR spectra are in agreement with the literature data.[2]

1-(2-Hydroxyphenyl)-3-(*p*-tolyl)propan-1-one (1b)

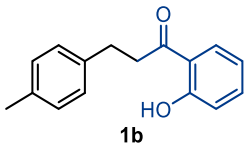

1b

Following the general procedure for the reductive alkylation with acetophenone derivatives using 47.0 µl of 4-methylbenzaldehyde (0.4 mmol) and 144.00 µL of 2′-hydroxyacetophenone (1.2 mmol) product **1b** was obtained in 70% NMR yield. The residue was purified by flash chromatograph InterChim PuriFlash, (eluent: ethyl acetate 98:2 for 20 min., Rf=0.24 in hexane: ethyl acetate 98:2 mixture) to afford 60.5 mg (63%) of the product as a colorless oil. The product is volatile.

^{1}H NMR (400 MHz, Chloroform-d) δ 12.35 (br s, 1H), 7.76 (d, *J* = 7.8 Hz, 1H), 7.48 (dd appears as t, *J* = 7.9 Hz, 1H), 7.18-7.13 (m, 4H), 7.00 (d, *J* = 8.3 Hz, 1H), 6.89 (dd appears as t, *J* = 7.5 Hz, 1H), 3.32 (t, *J* = 7.7 Hz, 2H), 3.05 (t, *J* = 7.7 Hz, 2H), 2.35 (s, 3H).
^{13}C NMR (101 MHz, Chloroform-d) δ 205.6, 162.6, 137.7, 136.4, 136.0, 130.0, 129.4, 128.4, 119.4, 119.0, 118.7, 40.3, 29.7, 21.1.
NMR spectra are in agreement with the literature data.[12]

4-(Naphthalen-2-yl)butan-2-one (1c)

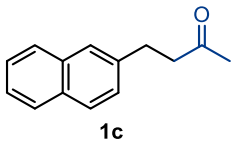

1c

Following the general procedure for the reductive alkylation with acetone using 63 mg of 2-naphthaldehyde (0.4 mmol) product **1c** was obtained in 68% NMR yield. The residue was purified by preparative thin-layer chromatography (eluent: hexane: ethyl acetate 7:2; Rf=0.60) to afford 48.1 mg (60%) of the product as a yellow oil.

^{1}H NMR (400 MHz, Chloroform-d) δ 7.84 – 7.75 (m, 3H), 7.64 (s, 1H), 7.46 (two t appears as p, *J* = 6.7 Hz, 2H), 7.34 (d, *J* = 8.3 Hz, 1H), 3.07 (t, *J* = 7.6 Hz, 2H), 2.85 (t, *J* = 7.6 Hz, 2H), 2.16 (s, 3H).

^{13}C NMR (101 MHz, Chloroform-d) δ 208.0, 138.6, 133.7, 132.2, 128.2, 127.7, 127.5, 127.1, 126.5, 126.11, 125.4, 45.1, 30.2, 30.0.
NMR spectra are in agreement with the literature data.[19]

3-(2-Chlorophenyl)-1-phenylpropan-1-one (1d)

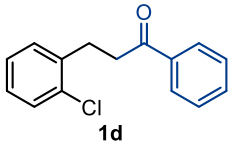

1d

Following the general procedure for the reductive alkylation with acetophenone derivatives using 45.0 µl of 2-chlorobenzaldehyde (0.4 mmol) and 140.00 µL of acetophenone (1.2 mmol) product **1d** was obtained in 70% NMR yield. The residue was purified by flash chromatograph InterChim PuriFlash, (eluent: ethyl acetate 97:3 for 20 min., Rf=0.30 in hexane: ethyl acetate 97:3 mixture) to afford 61.0 mg (63%) of the product as a colorless oil.

^{1}H NMR (400 MHz, Chloroform-d) δ 7.98 (d, *J* = 7.1 Hz, 2H), 7.56 (t, *J* = 7.4 Hz, 1H), 7.46 (dd appears as t, *J* = 7.6 Hz, 2H), 7.36 (dd, *J* = 7.5, 1.4 Hz, 2H), 7.25 – 7.12 (m, 1H), 3.32 (t, *J* = 7.8 Hz, 2H), 3.19 (t, *J* = 7.8 Hz, 2H).
^{13}C NMR (101 MHz, Chloroform-d) δ 199.1, 138.9, 136.8, 134.0, 133.2, 130.9, 129.7, 128.7, 128.2, 127.9, 127.1, 38.6, 28.4.
NMR spectra are in agreement with the literature data.[20]

3-(2-Chlorophenyl)-1-phenylpropan-1-one (1e)

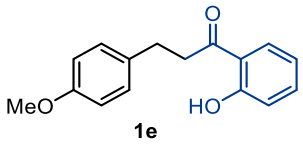

1e

Following the general procedure for the reductive alkylation with acetophenone derivatives using 49.0 µl of 4-methoxybenzaldehyde (0.4 mmol) and 144.00 µL of 2′-hydroxyacetophenone (1.2 mmol) product **1e** was obtained in 68% NMR yield. The residue was purified by flash chromatograph InterChim PuriFlash, (eluent: ethyl acetate 95:5 for 20 min., Rf=0.30 in hexane: ethyl acetate 95:5 mixture) to afford 61.8 mg (60%) of the product as a colorless oil.

^{1}H NMR (400 MHz, Chloroform-d) δ 12.34 (s, 1H), 7.75 (d, *J* = 7.9 Hz, 1H), 7.47 (t, *J* = 7.8 Hz, 1H), 7.18 (d, *J* = 8.6 Hz, 2H), 6.99 (d, *J* = 8.4 Hz, 1H), 6.91 – 6.83 (m, 3H), 3.80 (s, 3H), 3.30 (t, *J* = 7.7 Hz, 2H), 3.02 (t, *J* = 7.6 Hz, 2H).
^{13}C NMR (101 MHz, Chloroform-d) δ 205.6, 162.5, 158.2, 136.4, 132.8, 129.9, 129.4, 119.4, 119.0, 118.6, 114.1, 55.3, 40.4, 29.3.
NMR spectra are in agreement with the literature data.[21]

3-(2-Chlorophenyl)-1-phenylpropan-1-one (1f)

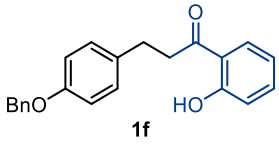

1f

Following the general procedure for the reductive alkylation with acetophenone derivatives using 85 mg of 4-(benzyloxy)benzaldehyde (0.4 mmol) and 144.00 µL of 2′-

hydroxyacetophenone (1.2 mmol) product **1f** was obtained in 62% NMR yield. The residue was purified by flash chromatograph InterChim PuriFlash (eluent: isocratic hexane: ethyl acetate 98:2 for 15 min., gradient hexane: ethyl acetate 98:2 → 95:5 for 1 min, isocratic hexane: ethyl acetate 95:5 for 15 min., Rf=0.3 in hexane: ethyl acetate 95:5 mixture) to afford 70.4 mg (53%) of the product as a colorless oil.

^{1}H NMR (400 MHz, Chloroform-d) δ 12.35 (s, 1H), 7.75 (d, J = 7.9 Hz, 1H), 7.50 – 7.32 (m, 6H), 7.18 (d, J = 8.5 Hz, 2H), 7.01 (d, J = 8.4 Hz, 1H), 6.94 (d, J = 8.6 Hz, 2H), 6.92 – 6.87 (m, 1H), 5.06 (s, 2H), 3.31 (t, J = 7.7 Hz, 2H), 3.03 (t, J = 7.6 Hz, 2H).
^{13}C NMR (101 MHz, Chloroform-d) δ 205.6, 162.6, 157.4, 137.2, 136.4, 133.1, 130.0, 129.5, 128.7, 128., 127.6, 119.4, 119.0, 118.7, 115.1, 70.2, 40.4, 29.3.
NMR spectra are in agreement with the literature data.[22]

3.4.3. ESI-MS study of catalytic mixtures

General procedure: A 10 mL screw-cap Schlenk tube was dried by Schlenk technique and charged with 10 mg [(*p*-cymene)$RuCl_2$]$_2$ (16 μmol, 1 equiv.), 69.2 mg of TBAT (128 μmol, 8 equiv.) or 35.5 mg of TBAC (128 μmol, 8 equiv.), then it was filled with carbon monoxide, 1 mL of THF was added. The Schlenk tube was sealed and heated for 4 hours at 160 °C. After that, the reaction mixture was cooled to room temperature, diluted in MeCN to achieve 0.1 mg/mL concentration, and analyzed by ESI-MS in both negative and positive modes. Positive mode mass spectra are blank, ruthenium-containing ions were detected only in negative mode spectra.

[(*p*-cymene)$RuCl_2$]$_2$ + CO

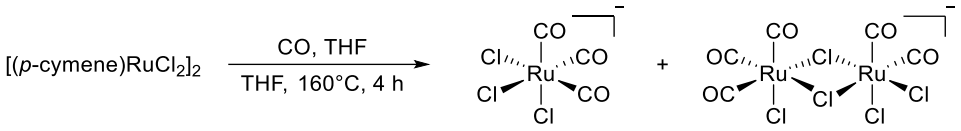

261.700: $Ru(CO)_2Cl_3^-$; 292.650: $Ru(CO)_3Cl_3^-$; 492.450: $Ru_2(CO)_4Cl_5^-$; 519.600: $Ru_2(CO)_5Cl_5^-$; 565.550: $Ru_2Cl_5(MeCN)(THF)_2^-$.

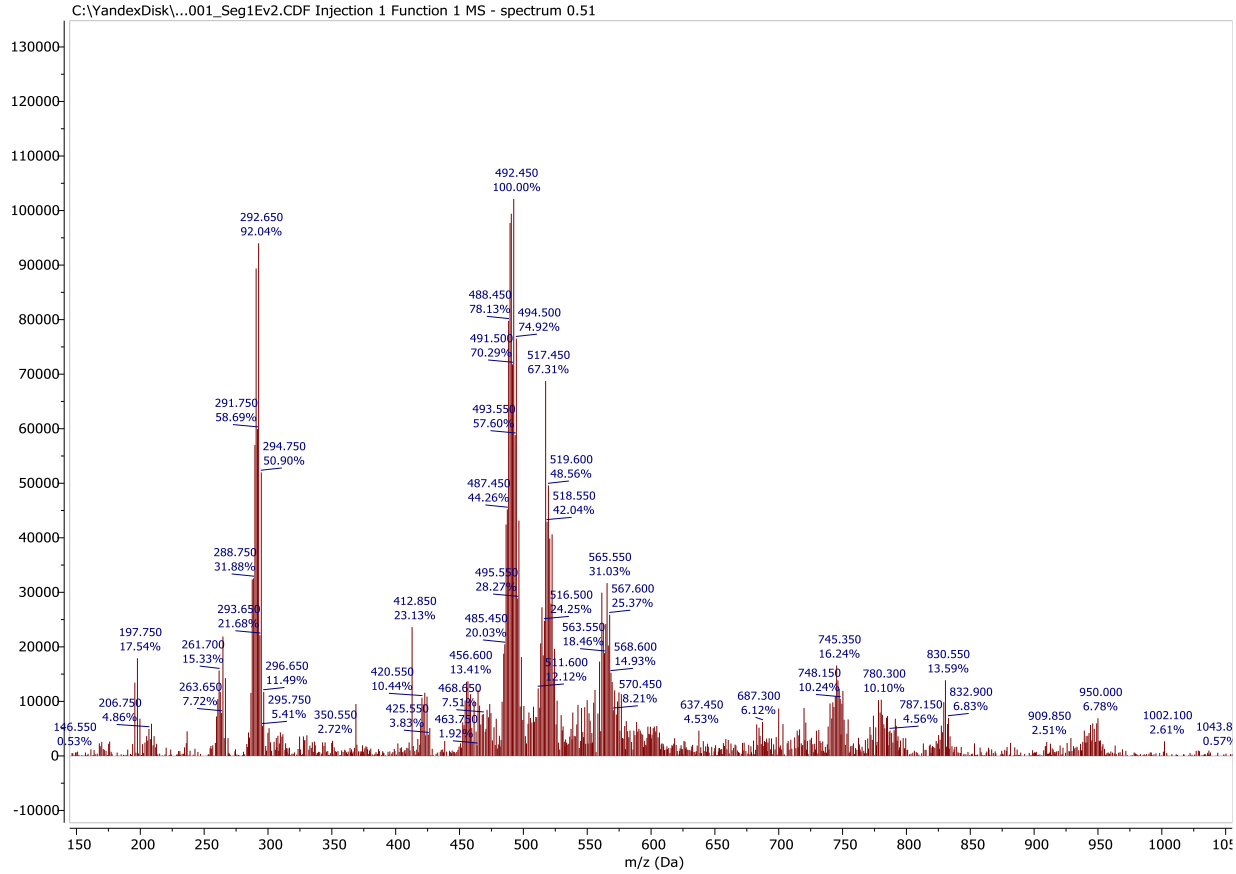

[(*p*-cymene)$RuCl_2$]$_2$ + CO + TBAT

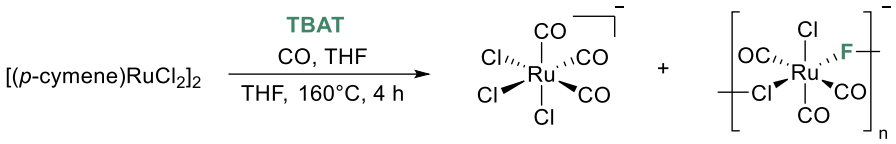

Some identified particles: 629.500: $Ru_2(CO)_8Cl_4F(MeCN)^-$; 741.400: $Ru_3(CO)_4Cl_5F_2(MeCN)(THF)^-$; 768.350: $Ru_3(CO)_2Cl_5F_2(MeCN)_3(THF)^-$; 863.600: $Ru_3(CO)_5F_7(MeCN)_7^-$;
911.200: $Ru_4(CO)_3Cl_6F_3(MeCN)_2(THF)^-$

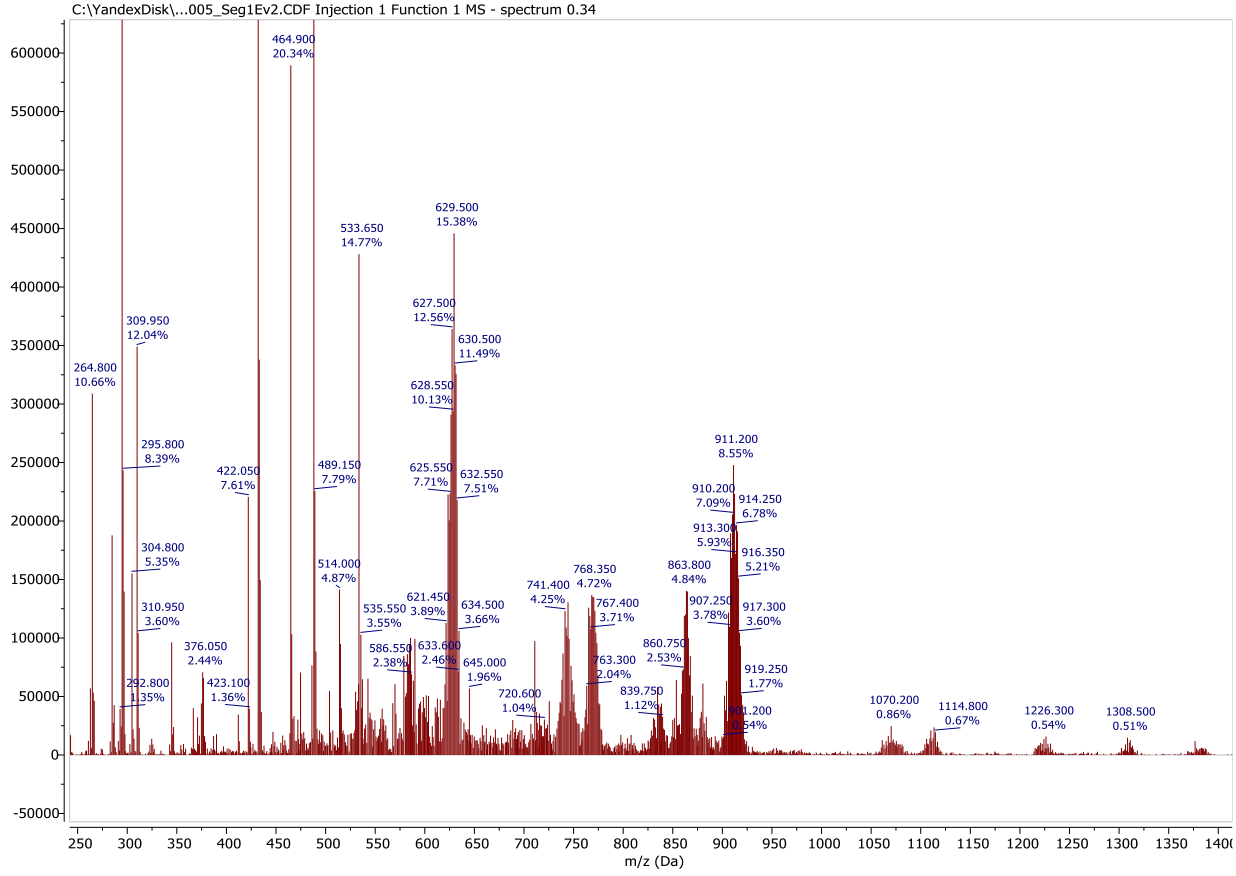

[(*p*-cymene)RuCl$_2$]$_2$ + CO + TBAC

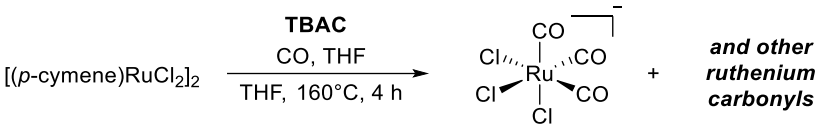

206.650: $RuCl_3^-$; 264.750: $Ru(CO)_2Cl_3^-$; 292.700: $Ru(CO)_3Cl_3^-$; 333.850: $Ru(CO)_3Cl_3(MeCN)^-$; $Ru(CO)_2Cl_3(THF)^-$; 629.600: $Ru_2(CO)_6Cl_5(MeCN)_2^-$; 768.650: $Ru_2(CO)_4Cl_6(Bu_4N)^-$; 823.700: $Ru_2(CO)_6Cl_6(Bu_4N)^-$

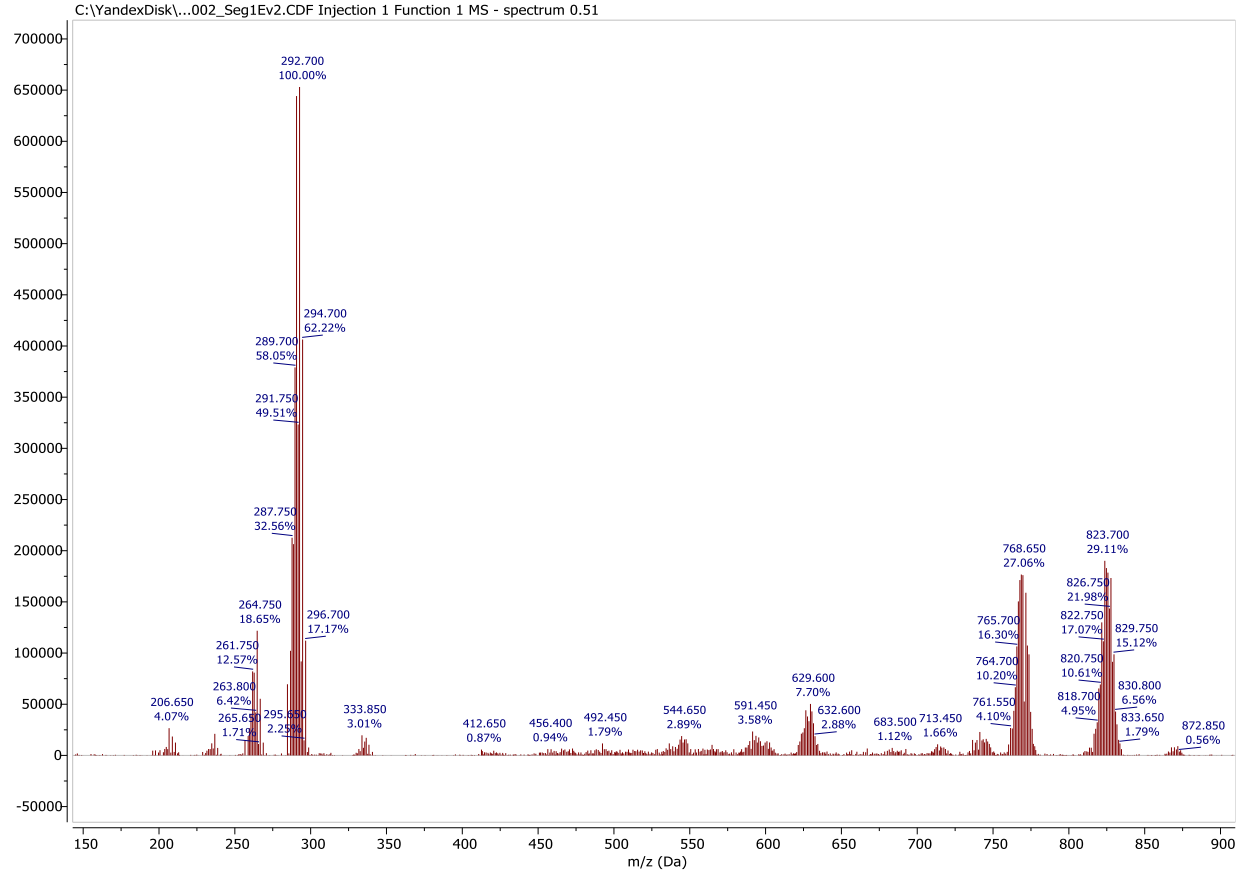

3.5. References

[1] S. Runikhina, D. Eremin, D. Chusov, *Chem. - A Eur. J.* **2021**, *27*, 15327–15360.

[2] S. A. Runikhina, O. I. Afanasyev, K. Biriukov, D. S. Perekalin, M. Klussmann, D. Chusov, *Chem. - A Eur. J.* **2019**, *25*, 16225–16229.

[3] S. E. Denmark, M. Y. S. Ibrahim, A. Ambrosi, *ACS Catal.* **2017**, *7*, 613–630.

[4] A. A. Tsygankov, M. Makarova, O. I. Afanasyev, A. S. Kashin, A. V. Naumkin, D. A. Loginov, D. Chusov, *ChemCatChem* **2020**, *12*, 112–117.

[5] F. Ferretti, D. Formenti, F. Ragaini, *Rend. Lincei* **2017**, *28*, 97–115.

[6] F. Ferretti, D. R. Ramadan, F. Ragaini, *ChemCatChem* **2019**, *11*, 4450–4488.

[7] J. W. Park, Y. K. Chung, *ACS Catal.* **2015**, *5*, 4846–4850.

[8] P. Zhou, C. Yu, L. Jiang, K. Lv, Z. Zhang, *J. Catal.* **2017**, *352*, 264–273.

[9] F. Ferretti, E. Barraco, C. Gatti, D. R. Ramadan, F. Ragaini, *J. Catal.* **2019**, *369*, 257–266.

[10] A. Ambrosi, S. E. Denmark, *Angew. Chemie - Int. Ed.* **2016**, *55*, 12164–12189.

[11] D. S. Pisal, G. D. Yadav, *Ind. Eng. Chem. Res.* **2020**, *59*, 2781–2795.

[12] B. M. Ivković, K. Nikolic, B. B. Ilić, Ž. S. Žižak, R. B. Novaković, O. A. Čudina, S. M. Vladimirov, *Eur. J. Med. Chem.* **2013**, *63*, 239–255.

[13] A. F. Hill, *Angew. Chemie Int. Ed.* **2000**, *39*, 130–133.

[14] A. R. Fatkulin, O. I. Afanasyev, A. A. Tsygankov, D. Chusov, *J. Catal.* **2022**, *405*, 404–409.

[15] C. Dalvit, C. Invernizzi, A. Vulpetti, *Chem. – A Eur. J.* **2014**, *20*, 11058–11068.

[16] A. Vulpetti, C. Dalvit, *Chem. – A Eur. J.* **2021**, *27*, 8764–8773.

[17] D. Chusov, B. List, *Angew. Chemie Int. Ed.* **2014**, *53*, 5199–5201.

[18] O. I. Afanasyev, A. A. Tsygankov, D. L. Usanov, D. S. Perekalin, A. D. Samoylova, D. Chusov, *Synth.* **2017**, *49*, 2640–2651.

[19] D. Zhang, T. Iwai, M. Sawamura, *Org. Lett.* **2019**, *21*, 5867–5872.

[20] S. Genç, S. Gülcemal, S. Günnaz, B. Çetinkaya, D. Gülcemal, *Org. Lett.* **2021**, *23*, 5229–5234.

[21] M. Soto, R. G. Soengas, H. Rodríguez-Solla, *Adv. Synth. Catal.* **2020**, *362*, 5422–5431.

[22] J. Hunter, S. Rice, R. Lowe, C. M. Pask, S. Warriner, V. Sridharan, *Tetrahedron Lett.* **2017**, *58*, 4400–4402.